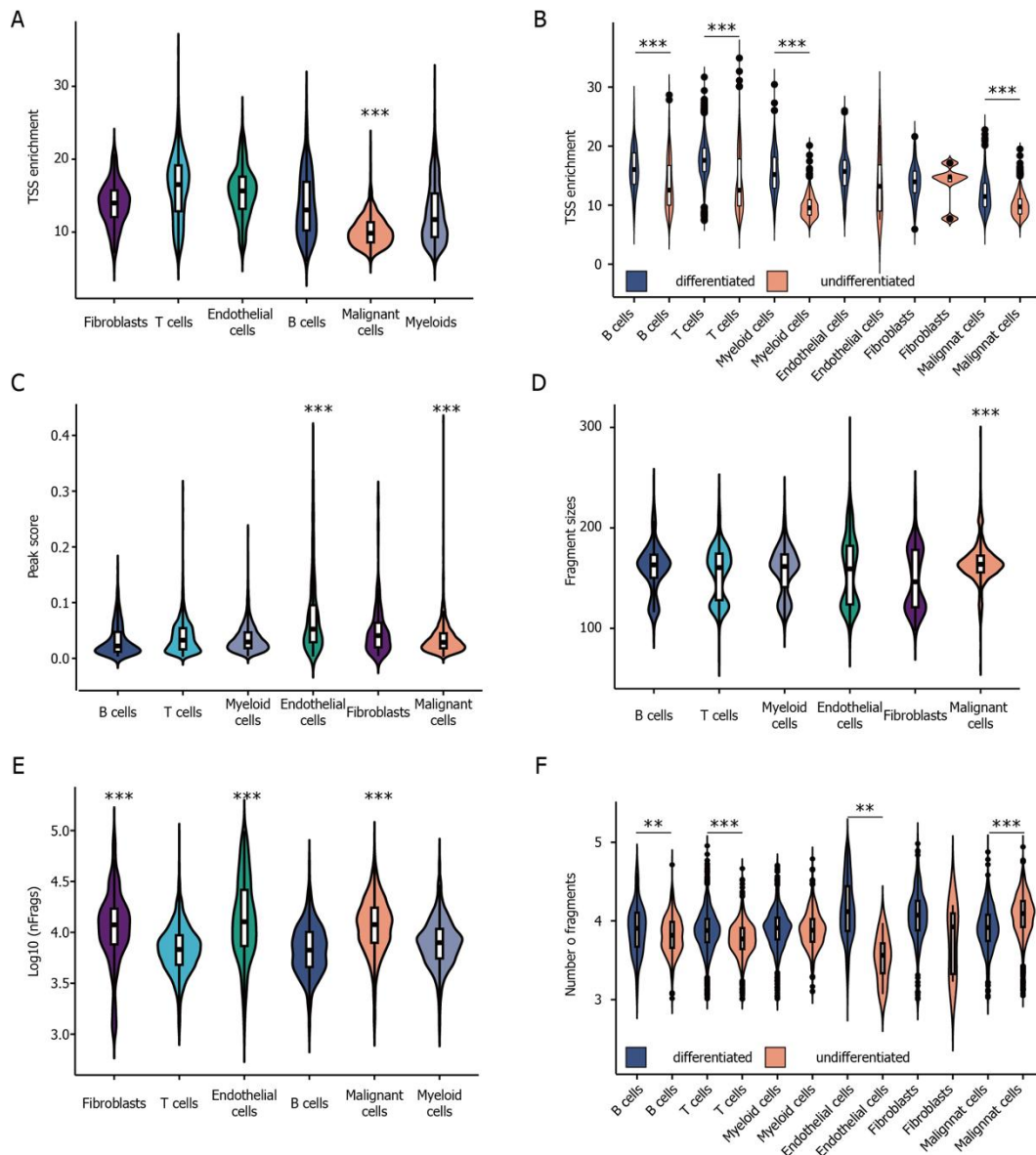


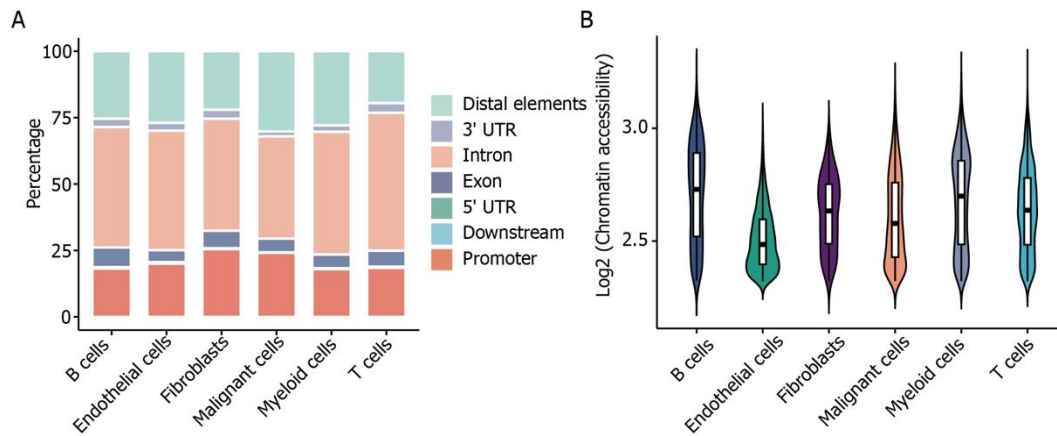
Supplementary Figure 1 Expanded view of matched scRNA-seq and scATAC-seq. A: Histogram of scATAC-seq inferred cell type prediction scores. The dashed vertical line in red at 0.5 represents a threshold cutoff for including cells in downstream analysis; B: Stacked bar charts showing contribution of each patient to each cell type in scRNA-seq; C: Stacked bar charts showing contribution of each patient to each cell type in scATAC-seq; D: Heatmap of inferred copy number variations (CNVs) by cell types.

Malignant clusters showed highest CNV burden; E: Violin plot show the distribution of CNV score for malignant cells stands for a statistically significant difference to other cell type in scRNA-seq; F: Violin plot show the distribution of CNV score for malignant cells stands for a statistically significant difference to other cell type in scATAC-seq.

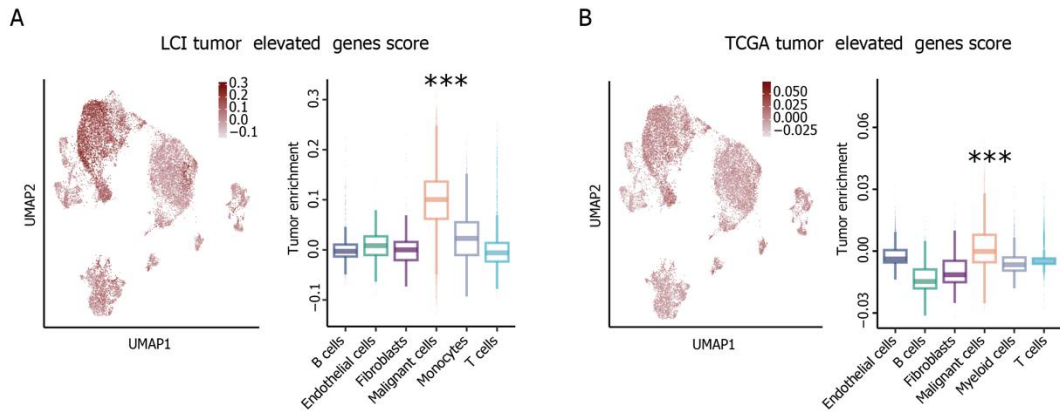


Supplementary Figure 2 Malignant cell chromatin accessibility exhibits distinct fragment profiles. A: Violin plot show the distribution of TSS enrichment score for malignant cells stands for a statistically significant lowest to other cell type in scATAC-seq ($P < 0.001$, Wilcoxon test); B: Differentiation-dependent TSS enrichment patterns. Undifferentiated tumors showed lower TSS scores in malignant cells ($P < 0.001$, Wilcoxon test); C: Violin plot show the distribution of peak score for malignant cells stands for a statistically significant high level to other cell type in scATAC-seq; D: Violin plot show the distribution of fragment sizes for malignant cells stands for a statistically significant high level to other cell type in scATAC-seq. E:

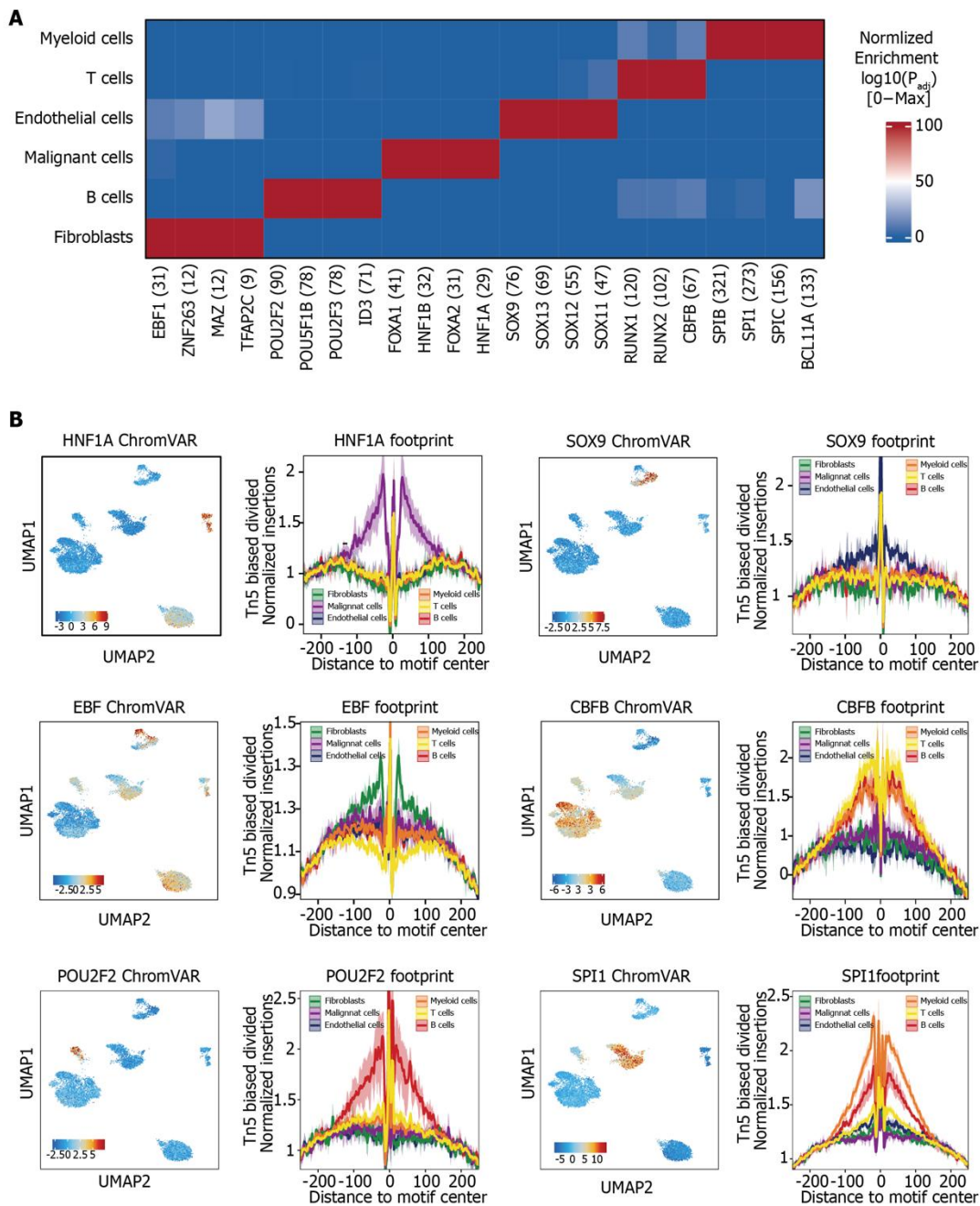
Fragment count per cell stratified by differentiation status. Undifferentiated tumors showed higher number of fragments in malignant cells ($P < 0.001$, Wilcoxon test); F: Violin plot show the number of fragments for malignant cells stands for a statistically significant high level to other cell type in scATAC-seq.



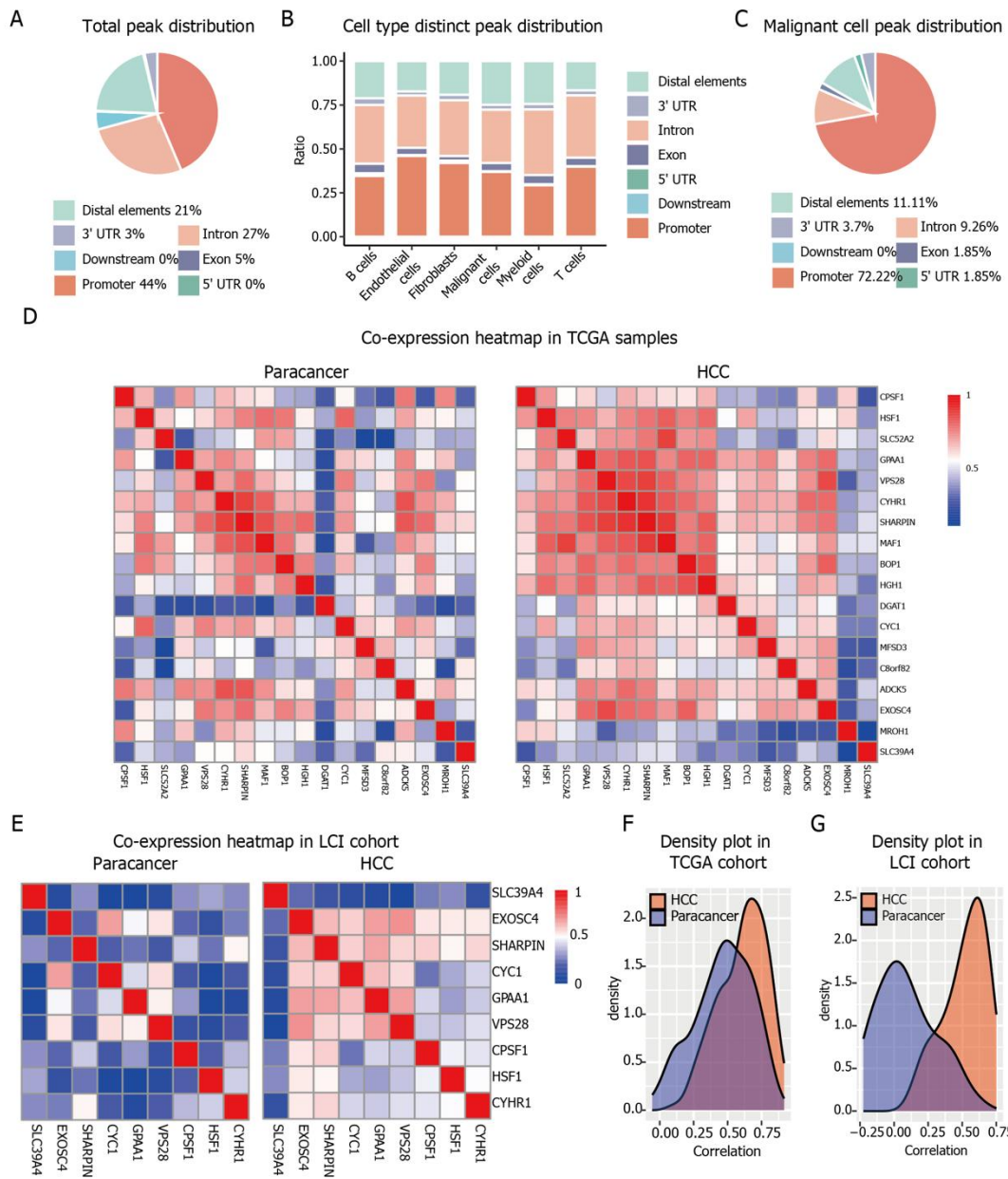
Supplementary Figure 3 Distribution of cell type specific elements identified in scATAC-seq. A: Proportions of cell type-specific accessible regions in promoter, intronic, and distal elements. Malignant cells and fibroblasts show promoter bias; B: Violin plot showing the distribution of score per peak for each cell type. Peaks in malignant cells showed slightly increased.



Supplementary Figure 4 UMAP plots of tumor elevated genes in scRNA-seq. A: UMAP plots of 15660 scRNA-seq cells color-coded by LCI tumor elevated genes enrichment score. Differential analysis was performed between the paired tumor and non-tumor samples. Genes with an FDR-adjusted p value less than 0.05 and a \log_2FC greater than 1 were considered tumor elevated genes; B: UMAP plots of 15660 scRNA-seq cells color-coded by TCGA tumor elevated genes enrichment score. Criteria for selecting tumor elevated genes remained same with LCI.

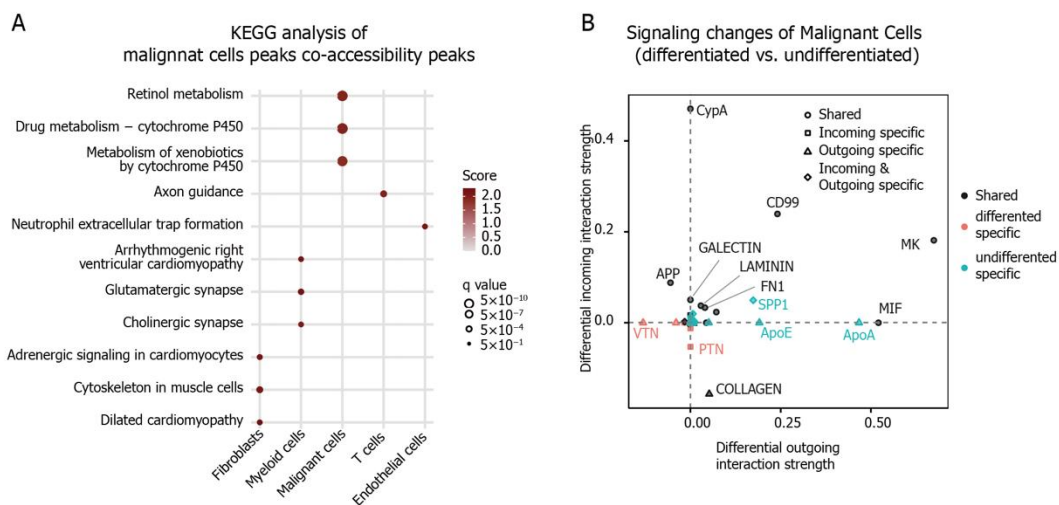


Supplementary Figure 5 Cell type specific transcription factors identified by scATAC-seq. A: Heatmap of top 4 transcription factors identified per cell type in scATAC-seq. Color intensity indicates enrichment scores; B: Bias estimates and average ATAC-seq signals centered around typical transcription factor per cell type.



Supplementary Figure 6 Expression of genes linked to the enhancer-like peak. A: Distribution of peak identified by peak-to-gene-links; B: Distribution of cell type specific peak identified by peak-to-gene-links; C: Distribution of malignant specific peak identified by peak-to-gene-links; each peak correlated with more than 8 genes; D: Co-expression heatmap of hub genes in adjacent non-tumor tissues (left) and paired tumor tissues (right) in the LCI cohort, demonstrating stronger co-expression patterns in tumor tissues; E: Kernel

density estimates show pairwise Pearson correlations among hub genes in tumor (red) versus adjacent non-tumor tissues (blue) in TCGA cohort. Tumor correlations are significantly higher (paired Wilcoxon test, $P < 0.001$); F: Kernel density estimates show pairwise Pearson correlations among chromatin hub genes in tumor (red) versus adjacent non-tumor tissues (blue) in LCI cohort. Tumor correlations are significantly higher (paired Wilcoxon test, $P < 0.001$).



Supplementary Figure 7 Epigenetic-regulated cancer cell signatures. A: Pathway analysis of the peak enriched genes for each cell type using the KEGG pathway database. The score indicated normalized enrichment scores and q value denote Benjamini-Hochberg-adjusted P values; B: Volcano plots depicting differentially enriched pathways identified by comparison undifferentiated tumor samples and differentiated tumor samples.

Supplementary Table 1 Patient demographics and tumor characteristics of bulk sequencing samples

Characteristics		<i>n</i>	TCGA	LCI	
			Number of paired bulk ATAC-seq and RNA-seq (<i>n</i> = 17)	Number of paired paracancer and HCC RNA-seq (<i>n</i> = 59)	Number of paired paracancer and HCC RNA-seq (<i>n</i> = 209)
Gender	Male		11	35	183
	Female		6	24	26
Age at index			62.8 ± 13.5	63.1 ± 15.7	51.0 ± 10.6
Primary diagnosis	Hepatocellular carcinoma, NOS		17	59	210
AJCC pathologic stage	Stage I		6	22	90
	Stage II		1	12	74
	Stage III		6	14	43
	Stage IV		0	1	0
	Not reported		4	10	2
Vital Status	Alive		8	18	130
	Dead		9	40	79
	Not reported		0	1	0

Supplementary Table 2 Patient demographics and tumor characteristics of single cell data

Sample	Diagnosis	Age	Gender	Race	Etiology	Stage	Grade	Local therapy	scATAC cells	scRNA cells
H38	HCC	74	Male	Asian	None	I	moderately differentiated	resection	1738	1046
H62	HCC	67	Female	White	HCV	I	well differentiated	resection	1818	519
H70	HCC	72	Male	White	Autoimmune hepatitis	II	Undifferentiated	resection	4813	7205
H77	HCC	72	Male	White	HCV	III	poorly differentiated	TACE	470	4800
H30	HCC	63	Male	White	HCV	IV	Undifferentiated	XRT (pancreas)	723	805
H65	HCC	62	Female	White	HCV	IV	unknown	None	216	589
H63	HCC	81	Male	Asian	HBV	IV	poorly differentiated	Ablation	278	545
H23	HCC	42	Female	White	NASH	IV	moderately differentiated	TACE	145	151

Supplementary Table 3 Genes increased by the strongest enhancer-like elements in malignant cells (Peak annotation: chr8:144313627-144314126)

	Gene symbol	Chr	Start	End	Correlation	FDR	VarQRNA	EmpPval
1	ADCK5	8	144373088	144393242	0.60585262	8.09789369187787e-49	0.78969512	0.03192565
2	BOP1	8	144262045	144291438	0.82307639	4.83837234294215e-119	0.93195122	0.0032154
3	CPSF1	8	144393231	144409335	0.81776004	2.9156126593125e-116	0.74353659	0.00342519
4	CYHR1	8	144449582	144462871	0.79018044	3.58784584455391e-103	0.85493902	0.00472727
5	EXOSC4	8	144064056	144080648	0.60042687	9.53449249360708e-48	0.78646341	0.03355886
6	GPAA1	8	144082634	144086216	0.8363305	2.10616590628857e-126	0.85926829	0.00274235
7	HGH1	8	144140851	144140851	0.69082482	9.75819589751336e-69	0.81323171	0.01394498
8	HSF1	8	144291604	144314720	0.80897682	7.32573948440087e-112	0.59506098	0.00379925
9	MAF1	8	144104461	144107611	0.8381976	1.71852485178062e-127	0.53256098	0.00268108
10	SHARPIN	8	144098637	144103773	0.8564401	6.28163911589334e-139	0.84878049	0.00214498
11	SLC52A2	8	144358552	144361272	0.81564057	3.53499053845465e-115	0.8595122	0.00351225
12	C8orf82	8	144525733	144529111	0.67071964	2.0213335750734e-63	0.80817073	0.01710053
13	CYC1	8	144095076	144097525	0.82900087	2.97705204794295e-122	0.96810976	0.00299544
14	DGAT1	8	144314584	144326852	0.88202108	6.10952342805177e-158	0.95786585	0.00155767

15	MFSD3	8	144509070	144511213	0.88190018	7.68461979270412e-158	0.9277439	0.00156006
16	MROH1	8	144148016	144261926	0.87610471	3.60990646849266e-153	0.99073171	0.00167854
17	SLC39A4	8	144412414	144416844	0.74001155	8.46178628795182e-84	0.65292683	0.00828926
18	VPS28	8	144423617	144428548	0.86093357	5.48987940781301e-142	0.91359756	0.00202898

Supplementary Table 4 Number of co-accessible peak across cell types

Cell 1	Cell 2	Total	Differentiated tumor	Undifferentiated tumor
Malignant cells	Malignant cells	11102	33014	6240
Malignant cells	Endothelial cells	391	621	407
Malignant cells	Fibroblasts	211	310	225
Malignant cells	B cells	55	214	44
Malignant cells	T cells	73	90	73
Malignant cells	Myeloid cells	183	327	273
Endothelial cells	Endothelial cells	1554	10832	146
Endothelial cells	Fibroblasts	56	417	31
Endothelial cells	B cells	10	30	19
Endothelial cells	T cells	22	37	23
Endothelial cells	Myeloid cells	391	303	290
Fibroblasts	Fibroblasts	520	5392	22
Fibroblasts	B cells	3	12	11
Fibroblasts	T cells	12	14	18
Fibroblasts	Myeloid cells	21	36	72
B cells	B cells	700	62	2204
B cells	T cells	31	127	68
B cells	Myeloid cells	29	251	81
T cells	T cells	2502	4402	2598
T cells	Myeloid cells	98	127	83
Myeloid cells	Myeloid cells	7520	16568	14608